DENTAL MATERIALS 34 (2018) 879–890

Available online at www.sciencedirect.com

ScienceDirect

journal homepage: www.intl.elsevierhealth.com/journals/dema

Aging resistance, mechanical properties and translucency of different yttria-stabilized zirconia ceramics for monolithic dental crown applications

E. Camposilvan[a,b], *R. Leone*[c], *L. Gremillard*[a], *R. Sorrentino*[c], *F. Zarone*[c], *M. Ferrari*[d], *J. Chevalier*[a,*]

[a] *Université de Lyon, INSA de Lyon, MATEIS CNRS UMR5510, 7 Av. Jean Capelle, 69621 Villeurbanne, France*
[b] *Department of Materials Science and Metallurgical Engineering, Universitat Politècnica de Catalunya, C/Eduard Maristany, 10-14, 08930 Barcelona, Spain*
[c] *Department of Neurosciences, Reproductive and Odontostomatological Sciences, Prosthodontic Area, University "Federico II", Napoli Italy*
[d] *Department of Prosthodontics and Dental Materials, University of Siena, V.le Bracci 1, 57100, Italy*

ARTICLE INFO

Article history:
Received 15 July 2017
Received in revised form
24 February 2018
Accepted 12 March 2018

Keywords:
Cubic zirconia
Hydrothermal degradation
Monolithic zirconia
Dental crown
Translucent zirconia
Aging

ABSTRACT

Objectives. The dental market moves towards high-translucency monolithic zirconia dental crowns, which are usually placed either with – or without – a thin glaze layer. The microstructural features and the mechanical performances of these materials are still controversial, as well as their susceptibility to aging. This paper aims at studying these aspects in the current generation of zirconia dental crowns showing different degrees of translucency.
Methods. Four different commercial zirconia materials were investigated, including one standard 'full-strength' 3Y-TZP and three grades with improved translucency. The microstructural features (phase composition and assemblage, grain size) were carefully studied, as well as mechanical properties (biaxial bending strength and indentation toughness), translucency and aging behavior (in autoclave at 134 °C). Aging was conducted on crowns with and without glaze to better represent clinical uses.
Results. Important differences are found in terms of microstructures among the materials in terms of cubic phase content and yttria in the tetragonal phase, leading to different optical, mechanical and aging resistance properties. We show that higher cubic phase content leads to better translucency and stability in water steam, but at the expense of strength and toughness. A compromise is always inevitable between translucency and aging resistance on one side and mechanical properties on the other side.
Significance.

- Even so called 'high translucent' zirconia ceramics tested in this work should be considered as medium translucency materials.
- Aging occurs in standard state-of-the-art dental zirconia and glazing does not fully avoid this issue. However, aging did not compromise strength even after prolonged duration.

* *Corresponding author.*
E-mail address: jerome.chevalier@insa-lyon.fr (J. Chevalier).
https://doi.org/10.1016/j.dental.2018.03.006

- Aging is null in the 'highly translucent' zirconia grades but at the expense of strength, which is then comparable to glass-ceramics.

1. Introduction

Among ceramic materials, polycrystalline tetragonal zirconia stabilized with 3 mol.% of yttria (3Y-TZP) has become one reference in dentistry, due to its excellent mechanical properties and good aesthetics thanks to its white color and tooth-like appearance [1]. Especially in terms of strength, 3Y-TZP is the only single-oxide ceramic that guarantees values above 1 GPa in bending, allowing the design of thin-walled and multi-unit restorations [2].

Nonetheless, when zirconia was introduced in the market, its opacity obliged dental technicians to apply several layers of veneering ceramics in order to increase the superficial translucency. Indeed, polycrystalline tetragonal zirconia exhibits moderate translucency: since the refractive index n is different along the main crystal axes of the tetragonal symmetry, both reflection and refraction occur at grain boundaries leading to a reduction of the light transmittance [3,4]. However, veneering is a sensitive and time-consuming procedure, eventually increasing the risk of chipping [1–5].

More translucent full-ceramic materials, based on leucite-reinforced glass-ceramics (first generation) and lithium disilicate (second generation) were then developed successfully, as competitive alternatives to zirconia in the anterior sites [6,7]. Even if the strength of these materials (approximately 350–400 MPa in the case of lithium disilicate) is much lower than 3Y-TZP, they can be used with little or no veneering, so offering in some cases a comparable performance for the same total wall thickness [7]. Some zirconia-reinforced lithium silicate glass-ceramics have been recently introduced for monolithic restorations and show an incremental but significant increase of their strength, with reported values of more than 400 MPa [8].

In the quest towards a higher translucency of zirconia restorations, novel zirconia grades have been developed and commercialized in the last years [9,10]. Moreover, pre-sintered blocks are both available as pre-shaded in several tonalities and multilayered with gradients of chroma and different degrees of translucency [11]. Thanks to the improved aesthetics, the restorations made with such materials can be placed without any veneering ceramic (a thin, few microns thick, glaze coating layer may be added in visible regions), allowing a further reduction of the restoration thickness. Moreover, such so-called 'monolithic/full-contour' restorations allow decreasing the risks of chipping, the prosthetic cost and production time [12].

Obtaining a higher translucency in zirconia can be pursued with several strategies: (a) reducing the residual porosity, for example by adding a glassy phase or some sintering additives [13] (b) refining the microstructure so that grain boundaries do not interfere with light, (c) increasing considerably the grain size so to have less grain boundaries [12], and/or (d) introducing significant amounts of cubic phase, which is optically isotropic and does not induce birefringence [4]. All these strategies can be found in different commercial zirconia with a claimed improved translucency. In particular, we may now find novel yttria-stabilized grades with a higher content of yttria, which in turns lead to a higher content of cubic grains [14]. However, not only do these microstructural variations imply substantial improvements in the overall optical performance of zirconia, but they also inevitably introduce noticeable changes in its mechanical properties and long-term stability, as recently shown by Zhang et al. [15]. Concerning long-term stability, it has to be reminded at this stage that (3Y-TZP) is known to be susceptible to the so-called 'hydrothermal degradation', a superficial aging phenomenon that may take place, depending on microstructure, composition and stress state, when the surface is exposed to humid environment and moderate temperatures, including those found in the human body [16]. This aging process consists in a slow tetragonal to monoclinic transformation of the grains at the surface in contact with water molecules [17]. This surface transformation is associated to the formation of uplifts on the surface and eventually micro-cracking and grain pull-out, which may induce a progressive deterioration of mechanical properties [18].

The first objective of this work is to better understand how newly developed 'highly translucent' zirconia grades are designed in terms of phase assemblage (cubic and tetragonal phase content) and grain size to meet the demand for monolithic translucent zirconia restorations. Special emphasis is given to novel so-called 'cubic' zirconia, which have a limited follow-up in terms of microstructure-properties relations, including aging assessment. It is also our aim to study the mechanical properties and aging resistance of these new zirconia grades in comparison with standard 3Y-TZP grades. Most of aging studies of dental restoration materials (and this applies to Ref. [15]) are generally done on flat lab-scale samples and literature is sparse concerning real restorations from current zirconia grades after a chair-side clinically-representative preparation, while surface preparation is known to have a potential effect on aging rates [19]. In order to go a step forward, aging studies were thus performed on real crowns, prepared in the same condition than for clinical use, with or without the presence of a thin glaze that is often used for aesthetical reasons.

The hypotheses of this work were therefore that:

Table 1 – Summary of specimens' labeling and preparation procedures.

Label	Commercial name	Category	Nominal Y_2O_3 content (mol.%)	Al_2O_3 content (wt%)	Heating	Hold	Cooling
ST	Aadva ST	Full-strength	3	0.2	8 °C/min to 900 °C + 10 °C/min to 1500 °C	2 h	8°/min to T_{amb}
EI	Aadva EI	Enhanced translucency	3	0.05			
NT	Aadva NT	High translucency	5.5	0.05		2 h	10 °C/min to T_{amb}
ML	Katana UTML	High translucency multi-layered	>6	Un-known	10 °C/min to 1550 °C	2 h	10 °C/min to T_{amb}

- Higher translucency in newly developed zirconia grades might be due to an increase in grain size and/or an increase of the cubic phase content,
- This change in microstructural features should modify their stability under moisture and their mechanical properties,
- The presence of a glaze in monolithic restorations may modify the aging process by providing a protection layer, if the glaze is able to cover the entire surface in contact with water.

2. Experimental

2.1. *Materials*

Four different commercial zirconia materials were studied:

- One conventional 'full-strength' 3Y-TZP grade "Aadva ST" (Standard Translucency – ST group),
- One with improved translucency "Aadva EI" (Enamel Intensive – EI group),
- One highly translucent and partially cubic "Aadva NT" (Natural Translucent – NT group),
- One highly translucent, partially cubic and multi-layered in chroma "Katana UTML" (Ultra Translucent Multi Layered).

All the materials were provided in the form of commercial pre-sintered 98.5 mm disks. The first three zirconia ceramics were provided by Aadva, GC Tech, Leuven, Belgium and the fourth one by Kuraray Noritake Dental Inc., Aichi, Japan. From these pre-sintered blocks, both full-contour molar-crowns and disks were prepared, according to the procedures described below.

2.2. *Sample preparation: experimental crowns and disks*

For each material, full-contour molar-crowns preforms were milled by CAD-CAM technology from the pre-sintered disks. To obtain these preforms, human, sound, intact mandibular third molars extracted for periodontal reasons were first prepared according to the following standardized preparation geometries: 0.5 mm circumferential chamfer placed 0.5 mm above the cementum-enamel junction, axial reduction of 1.2 mm, total occlusal convergence of 10°, occlusal reduction of 1.5 mm; all preparation angles were rounded. Each prepared tooth was then covered with a powder for digital scanning (Cerec Optispray, Sirona Dental, Salzburg, Austria) and three-dimensionally scanned by means of a laboratory optical digital scanner (GC Aadva Lab Scan, GC, Tokyo, Japan). The 3D shape of each tooth was digitized, so as to use it for the fabrication of CAD–CAM monolithic crowns by means of a CAD software (Exocad, DentalCAD, Exocad GmbH, Darmstadt, Germany). The following configuration of the digital dies was used: core minimal thickness 0.6 mm, cement layer spacing 0.05 mm, cement layer starting 1.3 mm from the finishing line.

The preforms were then sintered according to the manufacturer's specifications, as summarized in Table 1. One half of each crown was manually glazed with a glaze thickness ranging between 10 and 100 μm, while the other half was left uncoated (see Fig. 1). Two different glazes proposed commercially were used: CeraFusion (Komet), based on lithium disilicate, which was fired at 1005 °C during 15′, and Magic Glaze Flu, fired at 900 °C during 15′ (Wieland Zenostar, Ivoclar Vivadent).

Similarly, 20 disks 1.5 mm in thickness and 12 mm in diameter were also prepared with CAD-CAM technology from each material. GC discs were milled at the Aadva CAD-CAM Production Centre (GC Europe, Leuven, Belgium) while the Katana discs were milled with Roland DWX-50 milling machine (Roland DGA Corporation, Irvine, CA, USA). They were sintered under the same conditions as the crowns, so as to exhibit the same microstructure and phase assemblage. The specimens were prepared and wet-finished in a grinder/polisher machine with 600 grit paper until the experimental dimensions were obtained. Then, the specimens were wet-polished with 1200 and 2400 grit paper and mirror-polished with diamond pastes (down to 1-μm). At the end of the process, the roughness Ra was measured to be less than 20 nm. Finally, the specimens were ultrasonically cleaned in distilled water for 10 min before measurement procedure.

The disks were used for mechanical tests as well as for translucency measurement (after reducing their thickness to 1 mm in that case, and then with the same polishing procedure as described above). Fig. 1 shows the appearance under transmitted light of the 4 types of specimens, obtained with a stereoscope Olympus SZX 10 under the same illumination and background conditions.

2.3. *Methods*

The experimental crowns and disks underwent a series of characterization, as summarized in Table 2. Disks were used to characterize the grain size, phase assemblage and composition since grain size measurement and X-ray diffraction (XRD) analysis are more accurate on flat samples. They were also used to measure the mechanical properties (strength and indentation fracture toughness). On the other side, crowns were used to measure artificial aging kinetics in autoclave and

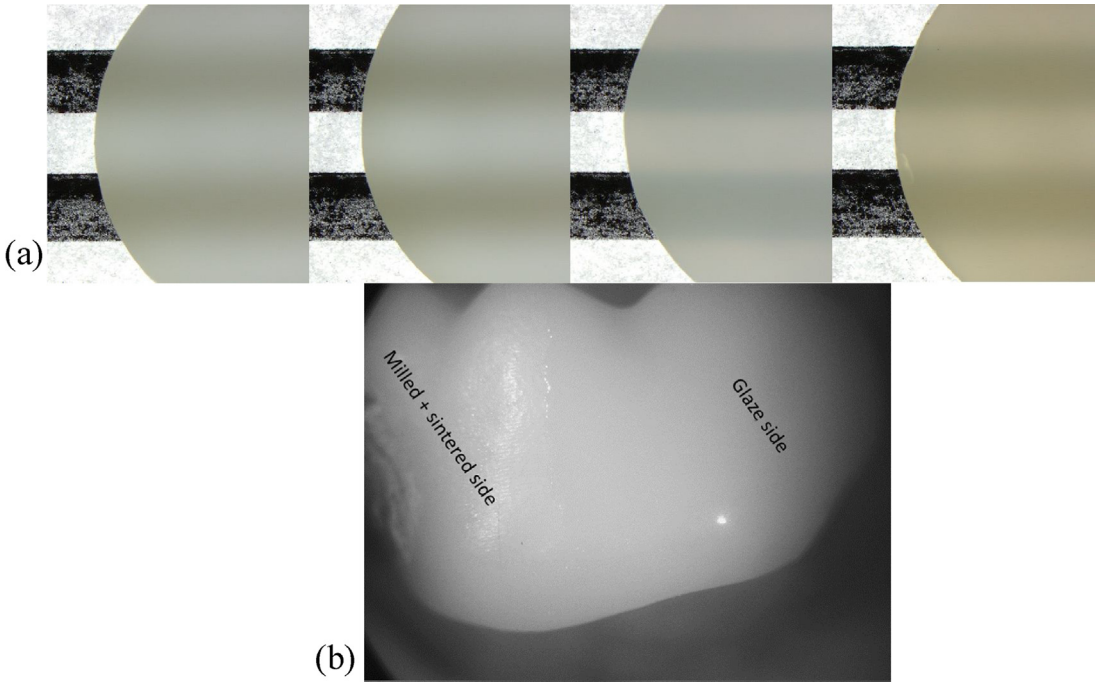

Fig. 1 – (a) Appearance of the 1 mm thick samples after polishing under transmitted light, obtained with a stereoscope Olympus SZX 10 under the same illumination, capture and background conditions. From left to right: ST, EI, NT, ML. (b) Image of a full-contour molar-crown, with one side glazed and the other not.

Table 2 – Summary of characterization methods conducted on experimental crowns or disks.

Sample geometry	Grain size Rietveld analysis	Translucency	Indentation fracture Biaxial strength	Aging kinetics in autoclave	Focused Ion Beam after aging
Crowns				X	X
Disks	X	X	X		

they were also inspected by Focused Ion Beam (FIB) after aging, as described below.

2.3.1. *Microstructure, phase assemblage and composition*

The microstructures were analyzed by scanning electron microscopy (SEM) on the disks surface after polishing and thermal etching at 1200 °C, 1 h.

XRD patterns were collected on disks and analyzed for different incident angle ranges with a Bruker D8 Advance equipment, using a CuKα radiation. 10–75° 2θ patterns were collected from polished disks to quantify the respective amount of tetragonal and cubic phases in the as-processed crowns by a Rietveld analysis employing the software Topas 4.0. The XRD diagrams were calculated using both cubic and tetragonal phases of zirconia. A first calibration of their lattice parameters versus Yttrium concentration [$YO_{1.5}$], using data from Scott [20,21] and from PDF files [22], showed that the lattice parameters vary as:

$2a_t.\sqrt{2} = 5.078495599 + 0.003767349\cdot[YO_{1.5}]$

$c_t = 5.192521486 - 0.002903167\cdot[YO_{1.5}]$

$a_c = 5.113195432 + 0.001731149\cdot[YO_{1.5}]$

Thus, in the tetragonal phase, a_t and c_t lattice parameters where constrained using the following equation:

$c_t = 9.10607452 - 1.08981088.a_t$

Rietveld calculation of the lattice parameters conducted using this method gave access to the yttria concentration in each phase. It also enabled to calculate the concentration of both cubic and tetragonal phases.

2.3.2. *Aging kinetics*

26–33° 2θ XRD scans were performed on crowns (both glazed and non-glazed) at level of the outer surface at time 0 and after 2, 6, 18, 54 h of artificial aging in autoclave (134 °C, 2 bar steam pressure). Such accelerated aging test in autoclave is proposed in the ISO 13356 standard on flat samples, up to 5 h duration [23]. In this work, our goal was to assess aging kinetics on the real final product (as aging may be sensitive to surface preparation) and up to longer duration, keeping in mind that one hour of such an accelerated treatment at 134 °C is roughly equivalent to 2–4 years at 37 °C [17]. The surface monoclinic content was quantified by measuring the areas of selected peaks and applying the formulas of Garvie and Nicholson [22] and Toraya et al. [24]. Between 26 and 33°, the volume fraction of monoclinic phase is given by:

$$V_m = \frac{1.311X_m}{1 + 0.311X_m},$$

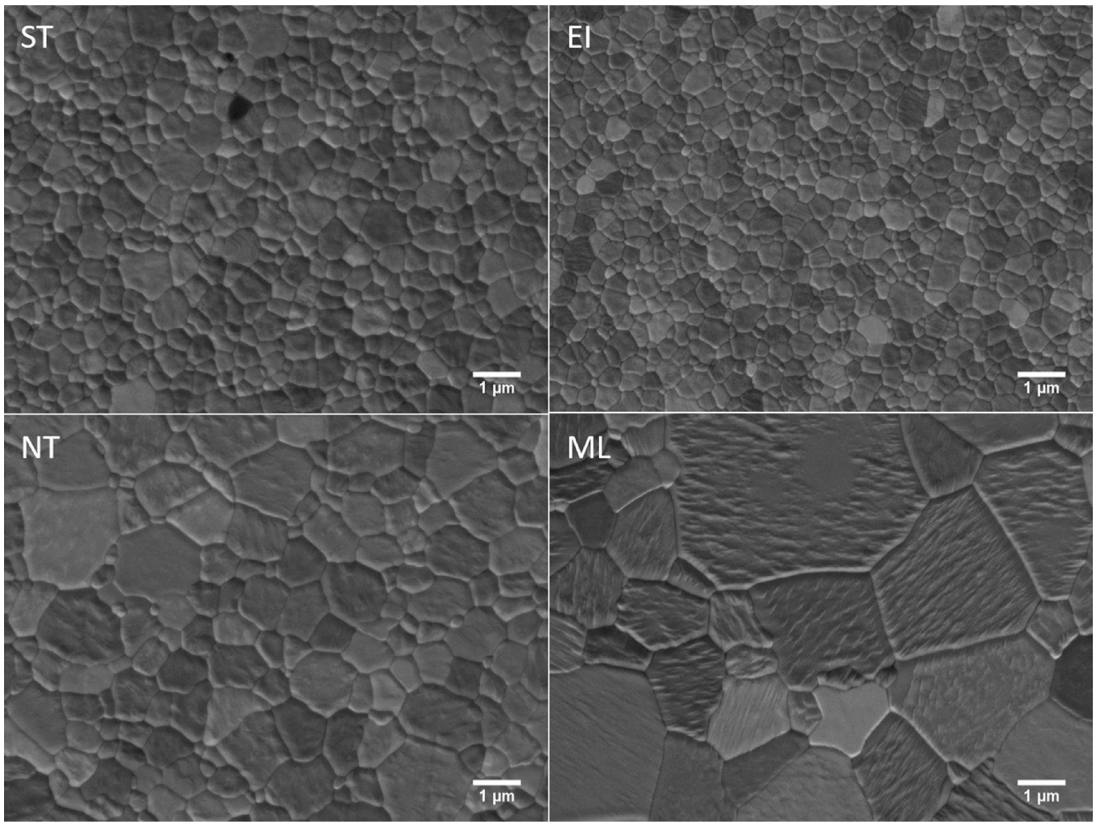

Fig. 2 – SEM images showing the microstructure of the 4 materials studied: ST, EI, NT, ML.

where

$$X_m = \frac{I_m^{\bar{1}11} + I_m^{111}}{I_m^{\bar{1}11} + I_m^{111} + I_t^{101}}$$

with I_p^{hkl} is the area of the diffraction peak of the phase p related to the plane (hkl).

When analyzing the glazed surface, a deeper penetration of the X-ray beam is needed. Thus XRD experiments were also performed at higher angles, between 53° and 65° 2θ.

In this case, the monoclinic fraction is calculated as:

$$V_m = \frac{R}{R + 0.26},$$

with

$$R = \frac{0.448A_4}{A_5 - A_6},$$

with:

$$A_4 = I_m(003) + I_m(221) + I_m(122) + I_m(310) + I_m(-311) + I_m(031) + I_m(-113) + I_m(-131)$$

$$A_5 = I_m(-222) + I_m(131) + I_m(-203) + I_t(103) + I_t(211)$$

$$A_6 = I_m(311) + I_m(-312) + I_m(113) + I_t(202)$$

These areas cover the respective angular range: $54° \leq A4 < 58°$; $58° \leq A5 < 61°$; $61° \leq A6 < 64°$. This method is based on the relative intensities of the above diffraction lines calculated in theoretical diffraction diagrams.

In order to study in details the local effect of a glazing on aging, Focused Ion Beam (FIB, nVision40 dual beam station – Carl Zeiss AG, Germany) was employed to cut and polish a trench between a glazed area and a non-glazed spot of selected aged crowns, after depositing a strip of protective Carbon. The sub-surface microstructure was then observed by Secondary Electron (SE) and backscattered (BSE) images, which can reveal the presence of phase transformation after a slight image treatment.

Measuring mechanical properties of crowns is possible, but is less reproducible than making simple biaxial testing and needs special caution in the analysis, especially when we are willing to obtain a strength data. Therefore, aging kinetics were measured on crowns but the effect of prolonged aging on the mechanical integrity of the materials was done on simple geometries. 10 ST and 10 EI disks were subjected to artificial degradation for 18 h in order to assess potential effect of a prolonged aging on biaxial bending strength, obtaining samples that were labeled, respectively, ST-A and EI-A. Indeed, only these materials were showing significant tetragonal to monoclinic transformation on experimental crowns (see Section 3).

2.3.3. *Mechanical and optical properties*

Biaxial strength was measured on disks by means of piston-on-three-balls strength tests, according to ISO 6872 standard using 10 disks per group. The fracture surface of aged materials was observed by SEM. Indentation fracture (IF) toughness and hardness tests were performed on polished disk surfaces

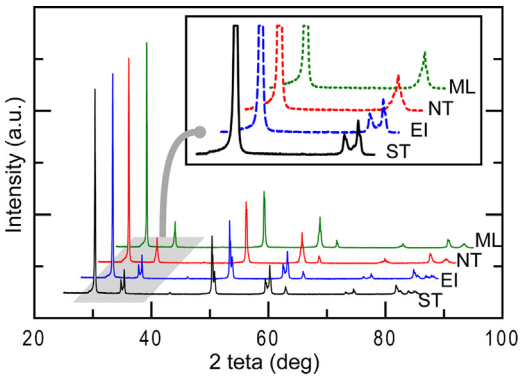

Fig. 3 – XRD representative patterns of the materials studied.

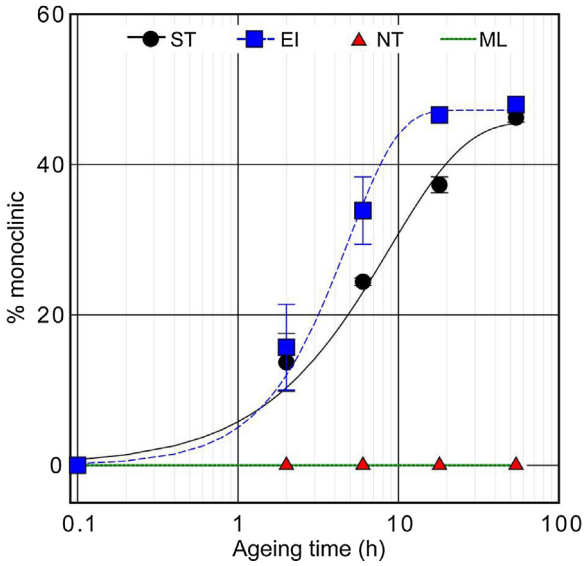

Fig. 4 – Evolution of the monoclinic content measured by XRD after artificial aging.

by using a Vickers indenter and an applied load of 10 kg for 10 s. The IF toughness values were calculated from the surface length of the cracks developing at the corners of Vickers indent using the formula proposed by Niihara [25]. These values are meant to have only a comparative significance, since this practical method presents several limitations, especially when applied to phase-transforming materials [26].

Total transmittance (Tt%) and Contrast Ratio (CR) were measured by a spectrophotometer (Jasco Y-670, France), on the disks after having reduced their thickness to 1 mm and fine polishing (1-μm diamond paste). The CR gives an indication of the opacity and is the ratio between the luminous reflectance of a specimen over a black background to that over a white background of a known reflectance. CR ranges from 0 (total translucency) to 1 (total opacity) [27]. The values measured at 555 nm wavelength were chosen to compare the different materials, according to the definition of the International Commission on Illumination [28].

The results were treated statistically with one-way analysis of variance (ANOVA) with a Tukey post-hoc test, employing the software Minitab. *p*-value was set at 0.05. Mean values plus standard deviations are presented in the results, while letters on the charts indicate the statistically significant differences.

3. Results

SEM images of the samples microstructure are shown in Fig. 2. The grain size, measured by the intercept method, is reported in Table 3. ST shows a classical grain size of 0.43 μm for a 3Y-TZP, while this value is reduced to 0.33 μm in EI. Both microstructures are quite homogenous, while a bimodal appearance is found in the highly translucent materials, where the grain size is much bigger, especially in ML.

The results of Contrast Ratio (CR) and total transmittance (Tt%) measurements are reported in the same Table 3, showing significant differences in both parameters. In order of increasing translucency, we find: ST, EI, ML, NT.

Fig. 3 shows XRD patterns taken from polished surfaces of the four materials before aging treatments. ST an EI have similar patterns representative of the tetragonal phase (doublets around $2\theta = 35^\circ$ and $2\theta = 60^\circ$), while in NT and ML the tetragonal doublets almost fuse together in single, large peaks. These large peaks are in fact triplets, constituted by the sum of tetragonal doublets and a single, dominant cubic peak between the doublets, representative of a large volume fraction of cubic phase. Due to the larger yttria content present in NT and ML tetragonal phase (thus a smaller tetragonality), the tetragonal peaks are less separated than in ST and EI. Rietveld analysis showed that all the materials are composed by a mixture of cubic and tetragonal phases, where approximately 30% of cubic phase is found in highly translucent crowns, and about 20% is found both in ST and EI materials, as indicated in Table 3.

The aging behavior of the four classes of materials is reported in Fig. 4, in terms of monoclinic volume fraction at the surface of the non-glazed side of the crown versus time.

NT and ML are fully resistant to phase transformation for the aging times applied here and no monoclinic content was observed even after prolonged duration. On the other side, ST and EI materials show significant phase transformation, starting from very short aging times (2 h). EI is aging faster than ST until 18 h of exposure, while they reach similar values at 54 h. It has to be considered at that stage that the penetration of the X-rays is about 5 μm in zirconia. Moreover, the monoclinic content obtained by XRD is a convoluted value for which the surface has a higher 'weight'. In other words, XRD captures the t-m transformation mostly from the first 1–2 μm. After 54 h of aging, it is logical to see a saturation of the monoclinic content, because this means that all the tetragonal grains have transformed on this 5 μm-thick layer.

Diffraction patterns taken from the glazed side of dental crowns were readable as well and allowed to measure the amount of monoclinic phase, since X-rays could generally penetrate through the glaze layer and reach zirconia surface. In some thicker glaze sections, 26–33° 2θ readings did not show zirconia peaks, meaning that the XRD beam did not reach the zirconia substrate for those angles. 53–65° 2θ were used in the latter case.

Table 3 – Grain size, phase analysis after Rietveld refinement and optical properties (CR and Tt%) for the four materials studied.

Grade	Grain size (nm)	Group	Tetrag. (%)	Cubic (%)	% Y_2O_3 in tetrag.	CR – group	Tt% – group
ST	432 ± 40	a	76.8	23.2	2.4	0.74 ± 0.01 a	36.9 ± 0.15 a
EI	333 ± 27	b	80.3	19.7	2.5	0.70 ± 0.01 b	38.4 ± 0.07 b
NT	770 ± 93	c	67.8	32.2	6.1	0.62 ± 0.01 c	43.4 ± 0.13 c
ML	1718 ± 327	d	68.9	31.1	5.9	0.69 ± 0.01 d	36.0 ± 0.07 d

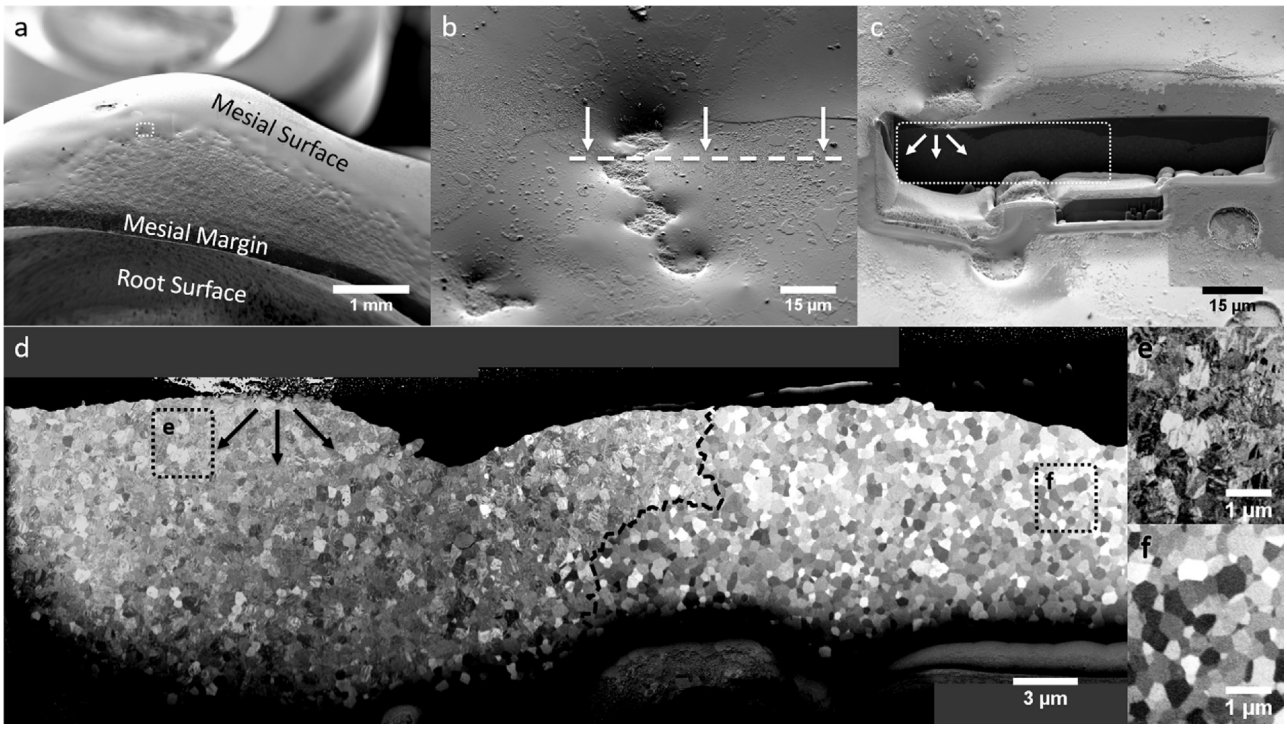

Fig. 5 – FIB study of an unglazed spot localized in the highlighted area of (a), in the mesial surface of an EI monolithic crown. The spot is observable at higher magnification in (b), where the line indicate the location of the trench, and the arrows the direction of FIB milling. In (c), the unglazed spot id visible to the left where the arrows indicate the direction of spreading of the degradation from the spot. The presence of glaze is also recognizable by the darker color with respect to the zirconia surface. By imaging the FIB trench with backscattered electrons, the transformed volume around the spot becomes clearly visible in (d). Unaffected microstructure is observable on the right side of the trench, well below the glazed region. The dashed line separates the aged and non-aged zirconia. Microstructural differences are illustrated in the detail pictures (e) and (f).

No monoclinic phase was found in any of the glazed zirconia ceramics, whatever the type of glaze ('CeraFusion' or 'MagicGlaze Flu'), even after prolonged aging exposure, except for some isolated cases. Optical microscopy observations revealed that in these cases a significant portion of the surface was left unglazed. The subsurface around some unglazed spots of an EI crown was therefore studied by FIB (Fig. 5) after 54 h artificial aging, where SEM analysis revealed that aging progressed from the exposed spot both towards the bulk and the sides, in a hemispherical volume of radius ~16 μm. At the same time, no aging was found at the interface zirconia-glaze beyond this distance.

Fig. 6 summarizes the mechanical properties obtained for the different materials. ST exhibit strength values well above 1000 MPa, while slightly lower values are reported for EI. For NT and ML the strength is similar, around 450 MPa.

Hardness was similar for the four materials tested, observing minor differences of less than 0.5 GPa. In order of increasing hardness, we find ST, EI, ML, NT. IF toughness was similar between ST and EI (~4.7 MPa$\sqrt{m}$) and significantly lower for both NT and ML (~3.8 MPa$\sqrt{m}$).

The biaxial strength did not show any variation after 18 h of artificial aging for ST-A materials, while results suggest a slight increase (even if not statistically significant) for EI-A samples. In the case of NT and ML materials, strength tests were not performed after aging since it was shown that these do not undergo any phase transformation for the applied hydrothermal exposure.

SEM observations performed on the fracture surface of 18hours-aged disks showed a mixed inter/transgranular appearance in the bulk region of both of them. Close to the surface that was put in tension during the strength test, the marked intergranular appearance produced by microcracking

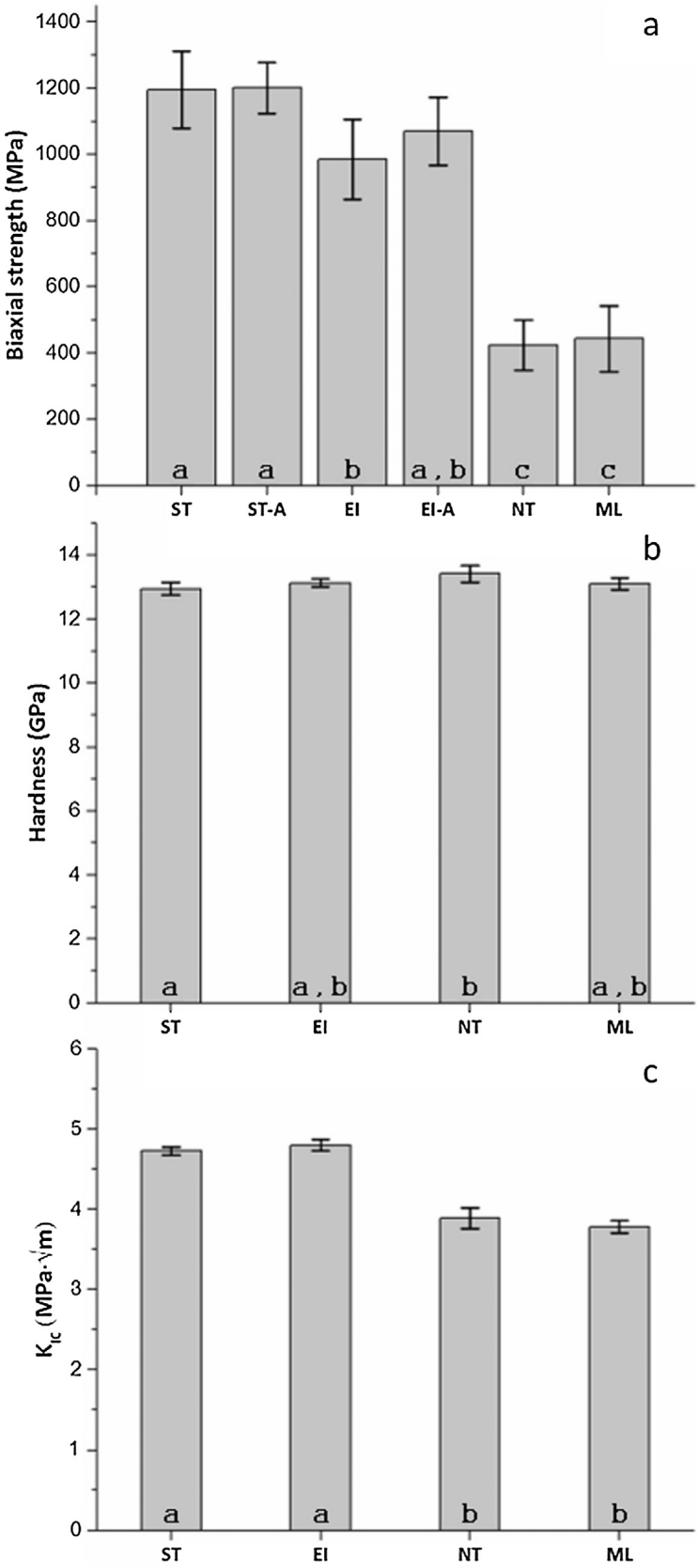

Fig. 6 – Biaxial strength before and after 18 h artificial aging for the four materials studied are reported in (a), where the suffix "–A" indicates aged materials. Hardness and IF toughness values are shown in (b) and (c), respectively. Letters indicate statistically significant differences.

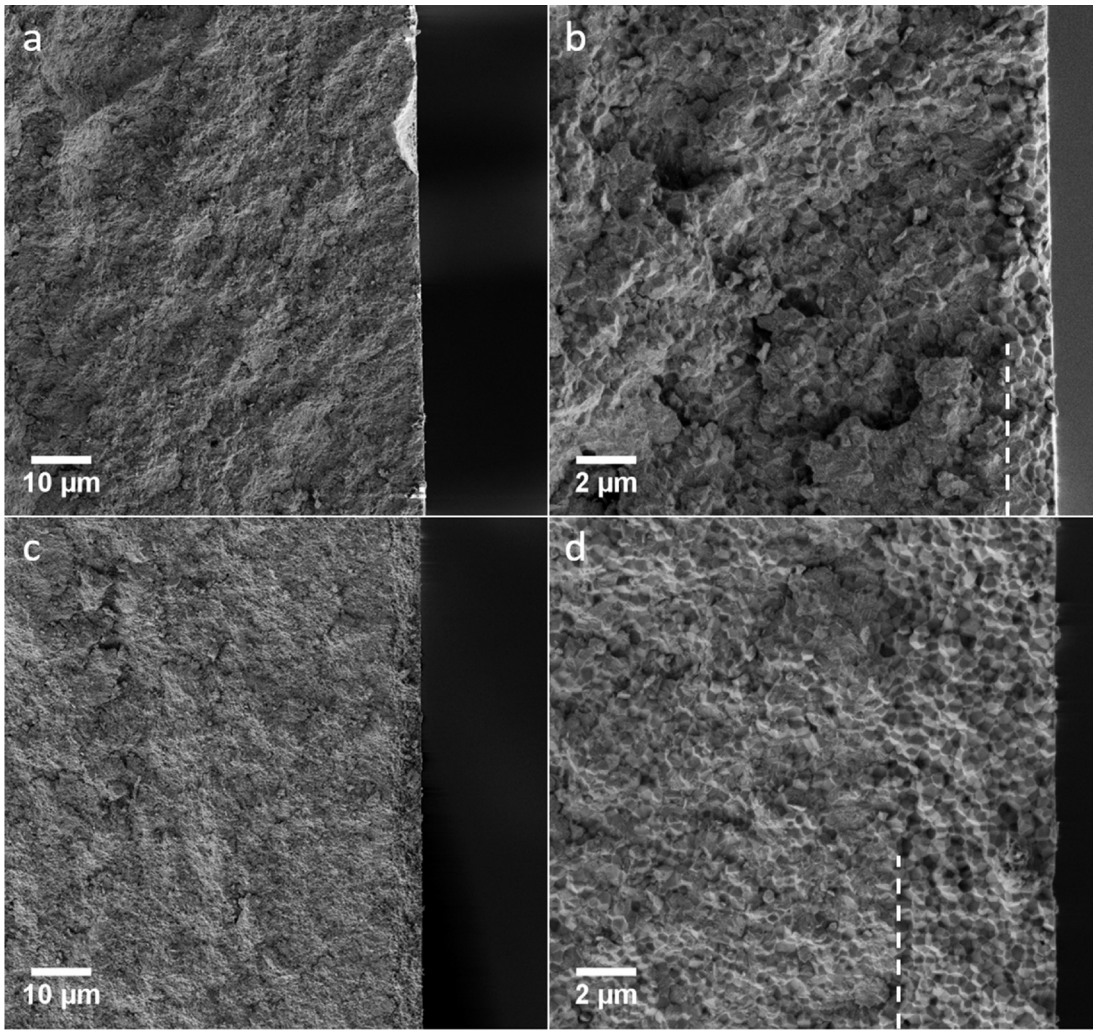

Fig. 7 – Fracture surface close to the tensile edge for ST-A (a, b) and an EI-A (c, d) representative samples, respectively. Dashed lines indicate the identified border between the intergranular appearance in the superficial aged layer and the mixed inter/transgranular appearance in the bulk.

in the aged layer was revealed, allowing to estimate its thickness, as shown in Fig. 7. This thickness was of ~2 μm for ST-A and of 5–6 μm for EI-A, respectively, which confirms previous XRD findings on the crowns: aging is significantly faster for EI samples than for ST samples either in the form of experimental crowns or disks.

4. Discussion

4.1. *Microstructure, composition & translucency*

Important differences are found in terms of microstructures among the materials studied. The first reason is indeed the yttria content, which is higher in NT and ML (at least ~5.5 mol.%) with respect to ST and EI (~3 mol.%). These additions allow obtaining a combined tetragonal-cubic microstructure (in agreement with the zirconia–yttria phase diagram [20,21]) where the translucency improvement should be twofold: cubic grains do not exhibit birefringence since they are optically isotropic; moreover, being the tetragonal grains supersaturated in yttria, their tetragonality is reduced and so are the refractive index and the amount of birefringence [4].

A difference in grain size and distribution exists between ML and NT, which can be attributed to the different sintering protocols. Their CR and Tt% is also significantly different, probably in relation to the presence of a chroma gradient in ML, as it has been shown in the case of colored and non-colored 3Y-TZP [29]. At the end, the potential better translucency of ML is not translated on measured Contrast Ratios (being quite similar to ST and EI).

The main differences between ST and EI are the grain size, which is smaller for EI, and the composition. Even if they have the same amount of yttria, the amount of alumina is substantially lower for EI (0.05 wt%). Alumina grains are randomly present in ST, like in other standard 3Y-TZP, due to the fact that tetragonal zirconia is generally supersaturated in alumina to improve its aging behavior and reinforce the grain boundaries [15,30]. An example is observable in Fig. 1a, where two alumina grains appear in darker shade. Therefore, the observed substantial improvement in CR and Tt% for EI when compared

to ST is justified by the absence of second phases (Al_2O_3) and smaller grains for EI. A reduction of the residual porosity might also justify the better optical properties for EI, since the presence of pores greatly affects light scattering. In fact, only some fractions % can lead to an opaque material, if the pores are bigger than approx. 50 nm [3].

Overall, the translucency of all the materials studied here is still below the one of enamel (CR ~0.45) and comparable to the one of dentine (CR ~0.65) for the more translucent ones. According to the classification introduced by Vichi et al. [31], all these materials can be classified as "medium-translucent" and their application as monolithic crowns in aesthetic frontal areas may find some limitations, even for NT and ML grades.

4.2. *Aging behavior*

The first and obvious evidence is that highly translucent zirconia with at least 5.5 mol.% yttria do not suffer from hydrothermal degradation even after 54 h of artificial aging. It can therefore be stated that these materials are fully resistant to aging under *in vitro* conditions and no external load applied. This implies that the tetragonal phase must be supersaturated in yttria with respect to 3Y-TZP, and so less transformable, as demonstrated by our Rietveld analysis. This is true for the thermal treatments applied here, while a similar behavior cannot be assured for longer sintering times or higher temperatures. In fact, the enhanced diffusion process in the latter case would promote a more complete separation of tetragonal and cubic phases, the cubic volume fraction would increase, pumping yttrium from the tetragonal phase, which would become less stable, and, eventually, vulnerable to hydrothermal degradation [32–34].

Another important point to underline is that hydrothermal degradation was observed in ST and EI starting from quite short aging times (2 h). Having EI smaller grain size than ST, a slower aging process could expected because of a lower transformability [35]. Nonetheless, the observed kinetics is faster for EI, which implies that the effect of alumina addition is more important than the difference in grain size, as reported in Refs. [15,36].

It is shown that glazing effectively protects 3Y-TZP against aging for the two glazes examined here and even for glazing thicknesses of few micrometers and 54 h of hydrothermal exposure. On the other hand, it was observed that a perfect glazing, coating 100% of the surface, is practically very difficult or even impossible to obtain. This can be the consequence of: (a) insufficient coverage during the glaze precursor application, especially for lithium silicate glazes that are applied by spray in form of powder, which tend to leave some unglazed spots in association with poor wetting during the application or de-wetting during thermal treatment (as suggested by Fig. 5) or difficulty of glaze application on the marginal edge; (b) chipping of the glaze, which may occur during cooling due to thermal residual stresses (associated to the fact that zirconia and the glaze do not exhibit the same thermal expansion coefficient). Therefore, if the material is susceptible to hydrothermal degradation, after glazing it will inevitably undergo the aging process in some localized areas, as it has been demonstrated by the FIB-SEM observations summarized in Fig. 5. Aging will spread from the non-glazed spot in radial direction, both towards the bulk and adjacent surface regions, so also below the glazed areas. The study was performed on an EI sample at 54 h exposure (i.e. the one aging faster after the more severe aging treatment) but one can expect qualitatively similar results for other 3Y-TZP grades. The first implication of this "pit aging process" is that one can expect the creation of subsurface micro-cracking and damage under the glaze, which may result in the risk of chipping due to the poor strength of degraded zirconia, especially when a tensile load is applied perpendicularly to the surface (separation load) [37]. This would, in turn, extend the unglazed spot, exposing neighboring areas to a similar phenomenon. A second implication is that this process creates damaged localized spots instead of a uniform degraded layer. While in the case of polished-and-aged zirconia the mechanical strength of 3Y-TZP is only slightly affected after long and severe hydrothermal exposure, the presence of these micro-cracked pits could lead to stress concentrations, which might have critical consequences especially in the marginal area. It could be interesting to further study the implication of this finding by looking at the influence of this 'pitting aging process' on the strength of aged samples.

4.3. *Mechanical properties*

The observed slight variations of hardness can be attributed to variations of microstructure and phase composition. It is well known from the Hall–Petch relation that, for the same composition, the smaller the grain size, the harder the material, as it happens for EI with respect to ST. NT is even harder due to the high amount of cubic phase, which is known to be harder than the tetragonal one [38]. ML has a lower hardness with respect to NT due to the bigger grain size, being the cubic phase content approximately equal for both.

Important differences were recorded in terms of biaxial strength, showing that ST and EI are at least twice as strong as NT and ML, implicating a high difference between full-strength and last generation highly translucent zirconia ceramics. This proves that the tetragonal phase in NT and ML is over-stabilized, having poor or no transformability for inducing the beneficial effects of the transformation toughening process. The biaxial strength for the presently studied highly translucent zirconia grades is just little better than for the best glass-ceramics available on the market, which are indeed more translucent [7]. Therefore, it is important for the dentist to avoid expecting a similar mechanical performance from both 'full-strength opaque' and 'translucent' zirconia ceramics. Both ST and EI fulfill the requirements for dental ceramics capable of supporting 4 and more units, even though the biaxial strength is slightly lower for EI. The difference in strength might be explained by the fact that smaller grain size means normally lower transformability, so EI is less mechanically transformable than ST. In addition, a more intergranular appearance was reported for fracture surfaces of 3Y-TZP with 0.05 wt% alumina with respect to compositions with 0.25 wt% alumina, meaning that in the latter grain boundaries are reinforced [36]. This aspect may also give a contribution to the observed strength difference.

No strength variation was recorded for ST after 18 h aging exposure, while a slight increase in the average strength was measured for EI. Although this difference is not significant, ST

and ST-A pertain to the same statistical group as EI-A, while EI does not. As demonstrated, both ST and EI are susceptible to hydrothermal t-m transformation, with ~35 Vm% and ~45 Vm%, respectively, recorded by XRD at 18 h. Although the monoclinic phase content measured by XRD in not very different (mainly because XRD only captures the very first microns of transformation, as discussed above), the thickness of aged and microcracked layer revealed by the fractographic images shown in Fig. 7 is significantly higher for EI-A samples. The different mechanical behavior can therefore have two possible justifications: (a) the aged layer induces some degree of "tip blunting" for the biggest defects/cracks naturally present in the material [39]: in this case, either the initial defects of EI are different in nature than the ones of ST and so more responsive to the blunting effect (bigger, sharper), or the higher amount of monoclinic phase in EI-A induces a deeper blunting effect; (b) since aging has progressed deeper in EI-A, the compressive layer which normally accompanies the aging process in the transition zone between degraded and non-degraded material is placed closer to the critical defects tip, inducing a reduction in their stress-intensity factor. These results show at the end that hydrothermal transformation does not induce necessarily a decrease in strength. The amount of strength degradation or improvement is dependent on compressive layer thickness versus defect size ratio and on the amount of micro-cracking in the process zone and any generalization would be un-correct.

IF toughness results support the above discussion, indicating sensibly lower values for NT and ML with respect to ST and EI. This difference can be interpreted as lower transformability for the highly translucent materials. On the other hand, IF toughness results were similar between ST and EI, so the difference in biaxial strength between the two groups may eventually be not imputable to a different mechanical transformability. Nonetheless, we prefer not to speculate further on this aspect due to the intrinsic limitations of the IF toughness test and its precision, which have been extensively discussed (disputed) by Quinn and Bradt [26].

4.4. *Clinical implications*

Some concerns surround the application of zirconia in dentistry due to the risk of hydrothermal degradation. In the present study, it has been shown that hydrothermal degradation takes place in state-of-the-art 3Y-TZP dental prosthetic applications prepared for clinical use. This phenomenon was not detrimental for strength in the studied materials, in these in vitro experimental conditions, even after long exposures. Although the possibility that cyclic functional or parafunctional loads could induce more severe – and maybe localized – aging process still remains an open question, these results are highly positive as far as the clinical use of zirconia dental restorations is concerned. Given the limitation of in-vitro studies to fully capture the complex clinical situation, future clinical studies and analyses of retrieved zirconia restorations after in vivo service, as proposed recently in Ref. [40], will be necessary to give a definite answer to this question.

On the other hand, the use of highly translucent, non-transformable zirconia materials should be carefully assessed. If it is true that these materials may be more translucent than standard 3Y-TZP and do not suffer from in vitro hydrothermal degradation, their toughness and strength are dramatically lower. Therefore, manipulation and crown preparation should be done carefully, avoiding thin walls and sharp edges as much as possible. Having similar (or little bit higher) mechanical strength than lithium disilicate glass-ceramics but lower translucency, the latter or novel options such as zirconia-reinforced lithium silicate glass-ceramic must still be considered as an alternative choice to these materials. Other aspects should however be taken in consideration as it is the case of dissolution and wear resistance to fully compare newly developed 'cubic' translucent zirconia and lithium disilicate in a global picture. Anyway, the term 'zirconia' must not hide the large diversity of microstructures and properties presented for this material's family today in the dental community.

Even if glaze acts as a barrier for the hydrothermal degradation, locations of un-complete glazing are always present (at least in the conditions of this study). Therefore, the glazing procedure does not represent a real protection against aging of the overall crown, so it should be considered only for aesthetical purposes.

5. Conclusion

In the current generation of the so-called 'tetragonal zirconia' monolithic crowns, hydrothermal degradation operates and can be observed for quite short aging times. Fortunately, at least in the in vitro conditions of this work, aging does not mean strength degradation, even for quite long duration and significant surface transformation. Glaze acts as a barrier against hydrothermal aging for the underlying zirconia; nonetheless glazing should not be considered as an absolute protection against aging, since some spots of the restoration surface are always left unglazed, especially in the marginal regions.

The presence of cubic phase in highly translucent materials entails two main advantages: a sensible increase in translucency and the complete absence of hydrothermal degradation. On the other hand, the lack of transformation toughening for cubic zirconia and the coarser microstructure cause a severe drop in mechanical properties, which can represent a limitation for their application in conditions where high mechanical stresses are applied.

REFERENCES

[1] Zarone F, Russo S, Sorrentino R. From porcelain-fused-to-metal to zirconia: clinical and experimental considerations. Dent Mater 2011;27(1):83–96.
[2] Denry I, Kelly JR. State of the art of zirconia for dental applications. Dent Mater 2008;24(March):299–307.
[3] Zhang Y. Making yttria-stabilized tetragonal zirconia translucent. Dent Mater 2014;30(10):1195–203.
[4] Klimke J, Trunec M, Krell A. Transparent tetragonal yttria-stabilized zirconia ceramics: influence of scattering caused by birefringence. J Am Ceram Soc 2011;94(6):1850–8.
[5] Ferrari M, Vichi A, Zarone F. Zirconia abutments and restorations: from laboratory to clinical investigations. Dent Mater 2015;31(3):e63–76.

[6] Denry I, Holloway JA. Ceramics for dental applications: a review. Materials (Basel) 2010;3:351–68.
[7] Zarone F, Ferrari M, Mangano FG, Leone R, Sorrentino R. Digitally oriented materials: focus on lithium disilicate ceramics. Int J Dent 2016, art. no. 9840594.
[8] Elsaka SE, Elnaghy AM. Mechanical properties of zirconia reinforced lithium silicate glass-ceramic. Dent Mater 2016;32(7):908–14.
[9] Fujisaki H, Kawamura K, Imai K. US2014227654A1: colored translucent zirconia sintered body and its use. 2014.
[10] Fujisaki H, Kawamura K, Imai K. EP2263988B1-light-transmitting sintered zirconia compact, process for producing the same, and use thereof. 2009.
[11] Yamada Y, Matsumoto A, Ito Y. US2016/0074142A1 – zirconia sintered body, zirconia composition and zirconia calcined body, production method of these, and dental prosthesis.
[12] Malkondu Ö, Tinastepe N, Akan E, Kazazoğlu E. An overview of monolithic zirconia in dentistry. Biotechnol Biotechnol Equip 2016;30(4):644–52.
[13] Anselmi-Tamburini U, Woolman JN, Munir ZA. Transparent nanometric cubic and tetragonal zirconia obtained by high-pressure pulsed electric current sintering. Adv Funct Mater 2007;17(16):3267–73.
[14] Shahmiri R, Standard OC, Hart JN, Sorrell CC. Optical properties of zirconia ceramics for esthetic dental restorations: a systematic review. J Prosthet Dent 2018;119(1):36–46.
[15] Zhang F, Inokoshi M, Batuk M, Van Meerbeek B, Vleugels J. Strength, toughness and aging stability of highly-translucent Y-TZP ceramics for dental restorations. Dent Mater 2016;32(12):e327–37.
[16] Haraguchi K, Sugano N, Nishii T, Miki H, Oka K, Yoshikawa H. Phase transformation of a zirconia ceramic head after total hip arthroplasty. J Bone Joint Surg Br 2001;83(7):996–1000.
[17] Chevalier J, Cales B, Drouin JM. Low-temperature aging of Y-TZP ceramics. J Am Ceram Soc 1999;82(8):2150–4.
[18] Chevalier J, Gremillard L, Deville S. Low-temperature degradation of zirconia and implications for biomedical implants. Annu Rev Mater Res 2007;37:1–32.
[19] Deville S, Chevalier J, Gremillard L. Influence of surface finish and residual stresses on the ageing sensitivity of biomedical grade zirconia. Biomaterials 2006;27(10):2186–92.
[20] Scott HG. Phase relationships in the zirconia–yttria system. J Mater Sci 1975;10:1527–35.
[21] Scott HG. Phase relationships in the yttira-rich part of the yttria–zirconia system. J Mater Sci 1977;12:311–6.
[22] Garvie RC, Nicholson PS. Phase analysis in zirconia systems. J Am Ceram Soc 1972;55(6):303–5.
[23] ISO 13356:2015 Implants for surgery – ceramic materials based on yttria-stabilized tetragonal zirconia (Y-TZP).
[24] Toraya H, Yoshimura M, Somiya S. Calibration curve for quantitative analysis of the monoclinic-tetragonal ZrO_2 system by X-ray diffraction. J Am Ceram Soc 1984;67(6). C-119-C-121.
[25] Niihara K. A fracture mechanics analysis of indentation-induced Palmqvist crack in ceramics. J Mater Sci Lett 1983;2(5):221–3.
[26] Quinn GD, Bradt RC. On the vickers indentation fracture toughness test. J Am Ceram Soc 2007;90(3):673–80.
[27] Powers JM, Dennison J, Lepeak P. Parameters that affect the color of denture resins. J Dent Res 1978;56(11):1331–5.
[28] CIE S 017/E:2011. International Lighting Vocabulary, Vienna, 2011.
[29] Pecho OE, Ghinea R, Ionescu AM, Cardona JC, Della Bona A, Del Mar Pérez M. Optical behavior of dental zirconia and dentin analyzed by Kubelka–Munk theory. Dent Mater 2015;31(1):60–7.
[30] Tsubakino H, Sonoda K, Nozato R. Martensite transformation behaviour during isothermal ageing in partially stabilized zirconia with and without alumina addition. J Mater Sci Lett 1993;12:196–8.
[31] Vichi A, Carrabba M, Paravina R, Ferrari M. Translucency of ceramic materials for CEREC CAD/CAM system. J Esthet Restor Dent 2014;26(4):224–31.
[32] Inokoshi M, Zhang F, De Munck J, Minakuchi S, Naert I, Vleugels J, et al. Influence of sintering conditions on low-temperature degradation of dental zirconia. Dent Mater 2014;30(June (6)):669–78.
[33] Chevalier J, Deville S, Münch E, Jullian R, Lair F. Critical effect of cubic phase on aging in 3 mol% yttria-stabilized zirconia ceramics for hip replacement prosthesis. Biomaterials 2004;25(November (24)):5539–45.
[34] Matsui K, Horikoshi H, Ohmichi N, Ohgai M, Yoshida H, Ikuhara Y. Cubic-formation and grain-growth mechanisms in tetragonal zirconia polycrystal. J Am Ceram Soc 2003;86(August (8)):1401–8.
[35] Becher PF, Swain MV. Grain-size-dependent transformation behavior in polycrystalline tetragonal zirconia. J Am Ceram Soc 1992;75(3):493–502.
[36] Zhang F, Vanmeensel K, Inokoshi M, Batuk M, Hadermann J, Van Meerbeek B, et al. Critical influence of alumina content on the low temperature degradation of 2–3 mol% yttria-stabilized TZP for dental restorations. J Eur Ceram Soc 2015;35(2):741–50.
[37] Camposilvan E, Torrents O, Anglada M. Small-scale mechanical behavior of zirconia. Acta Mater 2014;80:239–49.
[38] Gaillard Y, Anglada M, Jiménez-Piqué E. Nanoindentation of yttria-doped zirconia: effect of crystallographic structure on deformation mechanisms. J Mater Res 2009;24(3):719–27.
[39] Marro FG, Anglada M. Strengthening of vickers indented 3Y-TZP by hydrothermal ageing. J Eur Ceram Soc 2012;32:317–24.
[40] Koenig V, Wulfman CP, Derbanne MA, Dupont NM, Le Goff SO, Tang M-L, et al. Aging of monolithic zirconia dental prostheses: protocol for a 5-year prospective clinical study using ex vivo analyses. Contemp Clin Trials Commun 2016;4:25–32.